

γ -ray spectroscopy of the neutron-rich nuclei ^{89}Rb , ^{92}Y , and ^{93}Y with multinucleon transfer reactions

D. Bucurescu,¹ C. Rusu,^{2,3} N. Mărginean,^{1,2} C. A. Ur,^{1,4} G. de Angelis,² L. Corradi,² D. Bazzacco,⁴ S. Beghini,⁴ F. Della Vedova,² G. Duchene,⁵ E. Farnea,⁴ T. Faul,⁵ E. Fioretto,² A. Gadea,² W. Gelletly,⁶ B. Guiot,² M. Ionescu-Bujor,¹ A. Iordăchescu,¹ S. D. Landown,⁶ S. M. Lenzi,⁷ S. Lunardi,⁷ P. Mason,⁴ C. Mihai,¹ R. Mărginean,^{1,4} R. Menegazzo,⁴ G. Montagnoli,⁷ D. Napoli,² Zs. Podolyák,⁶ P. H. Regan,⁶ F. Scarlassara,⁷ A. M. Stefanini,² G. Suliman,¹ S. Szilner,^{2,8} M. Trotta,⁹ J. J. Valiente-Dobón,² and Y. H. Zhang¹⁰

¹National Institute for Physics and Nuclear Engineering, Bucharest, Romania

²INFN Laboratori Nazionali di Legnaro, Italy

³University of Texas at Dallas, School of Natural Sciences and Mathematics, Dallas, Texas, USA

⁴INFN-Sezione di Padova, Italy

⁵IN2P3/CNRS et Université Louis Pasteur, BP 28, Strasbourg, France

⁶Department of Physics, University of Surrey, Guildford, GU27XH, United Kingdom

⁷Dipartimento di Fisica dell'Università di Padova, Italy

⁸Ruder Bosković Institute, Zagreb, Croatia

⁹INFN-Sezione di Napoli, Università di Napoli "Federico II," Napoli, Italy

¹⁰Institute of Modern Physics, Chinese Academy of Sciences, Lanzhou, People's Republic of China

(Received 30 August 2007; published 4 December 2007)

The positive-parity yrast states in the ^{89}Rb , ^{92}Y , and ^{93}Y nuclei were studied using γ -ray spectroscopy with heavy-ion induced reactions. In the multinucleon transfer reactions $^{208}\text{Pb}+^{90}\text{Zr}$ (590 MeV) and $^{238}\text{U}+^{82}\text{Se}$ (505 MeV), several γ -ray transitions were identified in these nuclei by means of coincidences between recoiling ions identified with the PRISMA spectrometer and γ rays detected with the CLARA γ -ray array in thin target experiments. Level schemes were subsequently determined from triple- γ coincidences recorded with the GASP array in a thick target experiment, in the reactions produced by a 470 MeV ^{82}Se beam with a ^{192}Os target. The observed level schemes are compared to shell-model calculations.

DOI: [10.1103/PhysRevC.76.064301](https://doi.org/10.1103/PhysRevC.76.064301)

PACS number(s): 21.60.Cs, 23.20.Lv, 25.70.Jj, 27.60.+j

I. INTRODUCTION

The systematic behavior of the structure of neutron-rich nuclei with $N > 50$ in the mass $A \approx 90$ region, not far from the closed shell $N = 50$, is important to better understand the evolution of this shell gap as a function of proton number. However, for many of the nuclei in this region, information on the medium-high spin levels is scarce because of the difficulty reaching them via stable beam/target fusion-evaporation reactions. However, recent studies have shown that nuclei in this region can be studied by γ -ray spectroscopy in heavy-ion multinucleon transfer reactions: the $N = 50$ isotones [1] and the Se isotopes [2,3].

In the past decade there has been an increased interest in using quasielastic and deep-inelastic processes to populate and study a wide range of both projectile-like and target-like nuclei. To deduce the level scheme of a particular nucleus for which no γ transitions are previously known, one must first assign unambiguously transitions to the nucleus of interest that can be used as starting points in the construction of the level scheme by using the $\gamma\gamma$ coincidence technique (triple coincidences are preferable in case of a large number of γ -rays emitted in the reaction). In the present work, the first unambiguous assignments of transitions in the nuclei of interest were made in multinucleon transfer reaction experiments on thin targets where the recoiling ions were identified with good resolution using a large-acceptance spectrometer and coincidences

between the recoil nuclei and the emitted γ rays were also recorded. However, in such experiments, the statistics of the double or triple γ -ray coincidences are generally not enough for coincidence analysis and, consequently, another experiment using a multidetector γ -ray array and a thick target is necessary to achieve sufficient statistics in triple γ -ray coincidences. The correlated analyses of the final results obtained in such a combination of experiments lead in the current work to the identification of the previously unknown positive-parity yrast structures of the $N = 52$ nucleus ^{89}Rb and the $N = 53, 54$ nuclei $^{92,93}\text{Y}$.

The ^{89}Rb nucleus was studied previously using β^- -decay [4] and the (α, p) reaction [5] in which low-spin states were determined, with most of the states having limits for the spin value (see also the ENSDF evaluation [6]). The ^{92}Y nucleus was previously studied by β^- -decay [7] and the (d, α) reaction [8] (see also the ENSDF evaluation [9]). As a result, states with relatively low spins are known in this nucleus. In a similar way, low-spin levels in the ^{93}Y nucleus were studied using β decay [10] and isomeric transition (IT) decay [11], as well as by transfer reactions with light projectiles ($d, ^3\text{He}$) [12] and (p, α) [13] (see also the ENSDF evaluation [14]). The results of the present experiments complement the existing data with information on medium-high spin levels. A comparison of the experimental results with shell-model calculations is also presented.

II. EXPERIMENTS

A. Quasielastic and deep-inelastic reactions

Two experiments were performed using beams accelerated by the combination of the XTU Tandem and the superconducting LINAC ALPI accelerators at the Laboratori Nazionali di Legnaro. The first reaction was a 590 MeV ^{90}Zr beam of approximately 2 pnA on a $300\ \mu\text{g}/\text{cm}^2$ ^{208}Pb target deposited onto a $20\ \mu\text{g}/\text{cm}^2$ C backing, whereas the second reaction was a 505 MeV ^{82}Se beam of 4–6 pnA on a $400\ \mu\text{g}/\text{cm}^2$ ^{238}U target with a $20\ \mu\text{g}/\text{cm}^2$ C backing. The projectile-like ions were detected and identified with the PRISMA spectrometer [15] placed close to the laboratory frame grazing angle (56° for the first reaction and 64° for the second reaction, respectively) and having an opening of about 80 msr. In both cases, the γ rays were detected with the CLARA array [16]. Coincidences between the recoils and γ rays and between the γ rays were recorded in event mode and then processed off-line.

This technique allows unique assignment γ -ray transitions to particular nuclei by identifying the mass and atomic number of the reaction products detected in PRISMA. The mass spectra of the identified Rb ($Z = 37$) and Y ($Z = 39$) isotopes observed in the two reactions are displayed in Fig. 1, where a clear separation of different species is demonstrated. In the $^{90}\text{Zr}+\text{Pb}$ reaction, the nuclei studied in this work were mainly populated in multinucleon transfer processes [17,18], whereas in the $^{82}\text{Se}+\text{U}$ reaction there was also an important contribution from fission, as expected.

The coincidence relationships between the γ -ray transitions and the recoil nuclei were first investigated to associate unambiguously certain γ -ray transitions with the de-excitations of the nuclei of interest. To construct the level schemes of these nuclei, γ - γ coincidences (double or triple) are necessary, which are not provided with sufficient statistics by the thin target experiments with the CLARA-PRISMA setup. We have therefore used a different set of γ - γ coincidence data (acquired

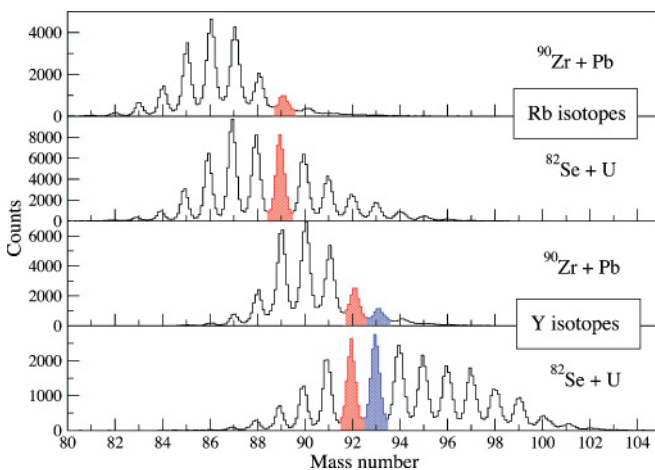


FIG. 1. (Color online) Mass spectra of the Rb and Y isotopes, as observed with the PRISMA spectrometer in coincidence with the CLARA γ -ray array, in the $^{90}\text{Zr}+^{208}\text{Pb}$ and $^{82}\text{Se}+^{238}\text{U}$ reactions, respectively. The hatched peaks correspond to the nuclei studied in this work.

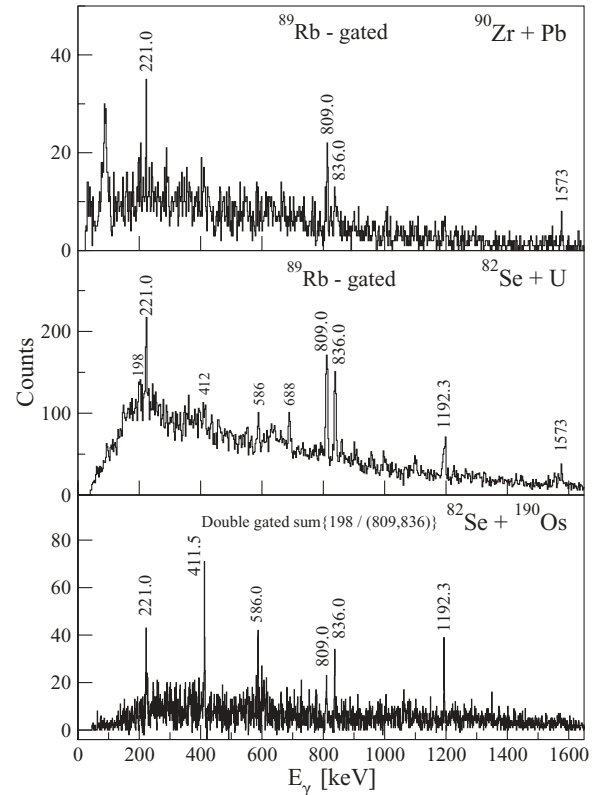


FIG. 2. (Upper panels) γ -ray spectra coincident with the mass peaks of ^{89}Rb shown in Fig. 1, in the two thin target multinucleon transfer reactions. (Lower panel) Triple coincidence γ -ray spectrum in the thick target experiment (see text, Sec. II B), with double gates as indicated, on transitions assigned to the yrast line of ^{89}Rb . The level scheme built from these data is shown in Fig. 3.

in another experiment performed on a thick-target) to deduce the level schemes.

B. Thick target experiment

The experiment used here has been described in a number of previous articles, for example, Refs. [2,3,19]. It was initially designed as a multinucleon transfer reaction experiment using a 470 MeV ^{82}Se beam on a $50\text{-mg}/\text{cm}^2$ -thick ^{192}Os target with a 0.2-mm-thick Ta backing. The nuclei of interest for the present work were populated mainly in deep-inelastic processes and possibly, as described in Ref. [20], via the fusion-evaporation reactions of the ^{82}Se beam with the ^{16}O contaminant of the oxidized target.

In this experiment, the reaction γ rays were detected with the GASP array [21]. In the off-line processing of the data, in addition to the regular two- and three-dimensional symmetrized γ -coincidence matrices, a number of asymmetric matrices were constructed to extract information on the multipolarity of the transitions. The asymmetric $\gamma\gamma$ coincidence matrices were sorted so that the energy signals from all detectors were histogrammed onto one axis and those from a specific ring of detectors at a given angle were counted along the other axis. Gating on the all-detector axis, the resulting spectra have the angular distribution (ADO) information

TABLE I. Experimental γ -ray transitions for the nuclei studied in this work, with their properties and assignment. The intensities are those from the spectrum coincident with the recoiling ions, in the $^{82}\text{Se}+^{238}\text{U}$ reaction (Fig. 2, Fig. 5, Fig. 7).

E_γ (keV)	E_i (keV)	E_f (keV)	J_i^π	J_f^π	I_γ	R_{ADO}^a	Character
^{89}Rb							
197.9(2)	1195.4	997.5	(9/2 ⁺)	(7/2)		0.80(8)	D
221.0(2)	221.0	0	(5/2 ⁻)	3/2 ⁻	29(8)	0.82(9)	D
411.5(2)	997.5	586.0	(7/2)	(7/2)		0.95(22)	D
586.0(3)	586.0	0	(7/2)	3/2 ⁻	16(6)	1.26(23)	Q
809.0(2)	2004.4	1195.4	(13/2 ⁺)	(9/2 ⁺)	100(8)	1.29(10)	Q
836.0(3)	2840.4	2004.4	(17/2 ⁺)	(13/2 ⁺)	84(8)	1.27(24)	Q
974.4(2)	1195.4	221.0	(9/2 ⁺)	(5/2 ⁻)		1.21(30)	(Q)
1192.3(4)	4032.7	2840.4	(19/2,21/2)	(17/2 ⁺)	53(13)	0.98(7)	(D,Q)
^{92}Y							
185.0(2)	185.0 + x	x			118(27)	0.56(7)	D
717.1(3)	4047.9 + x	3330.8 + x			108(17)	1.94(43)	Q
1022.8(2)	2304.3 + x	1281.5 + x				1.18(12)	Q
				1025 keV:	223(24)		
1026.5(5)	3330.8 + x	2304.3 + x				0.89(14)	D
1096.5(3)	1281.5 + x	185.0 + x			100(13)	1.27(13)	Q
^{93}Y							
291.4(2)	3636.8	3345.4	(21/2 ⁺)	(19/2 ⁺)	31(6)	0.77(7)	D
677.2(3)	4314.0	3636.8		(21/2 ⁺)	24(8)	1.16(27)	(Q)
722.6(3)	3345.4	2622.8	(19/2 ⁺)	(15/2 ⁺)	44(8)	1.50(19)	Q
791.7(2)	1550.4	758.7	(13/2 ⁺)	(9/2 ⁺)	100(8)	1.16(12)	Q
1072.4(3)	2622.8	1550.4	(15/2 ⁺)	(13/2 ⁺)	81(14)	0.93(19)	(D)

^aADO ratio determined from summed spectra conveniently gated on other transitions of the nucleus.

independent of the gating transition(s). We have constructed ADO (angular distribution from oriented states) ratios R_{ADO} as the total intensity of the transition observed in the rings at 35° and 145° divided by the intensity at 90°. Typical R_{ADO} values in this configuration are about 0.7 and 1.30 for pure dipole and quadrupole multiplicities, respectively.

III. RESULTS

A. The ^{89}Rb nucleus

The γ rays observed in coincidence with the ^{89}Rb mass peak (Fig. 1) are shown in the two upper panels of Fig. 2. The spectra observed in the two reactions show essentially the same γ rays. Strong γ rays at 809.0, 836.0, 1192.3, and 1573 keV (the last one is not currently placed in the level scheme) are the best candidates for the yrast transitions in this nucleus. The 221.0 keV γ ray, also clearly seen in both reactions, is the previously reported (5/2⁻) \rightarrow 3/2⁻ (g.s.) transition [6]. In the $^{82}\text{Se}+\text{U}$ reaction spectrum, shown in the middle panel of Fig. 2, other previously reported transitions with energies of 197.9, 411.5, and 586.0 keV, which originate from the low-energy states [6] can be observed with weak intensities.

The relationships between γ rays were studied using a triple $\gamma\gamma\gamma$ coincidence cube from the $^{82}\text{Se}+^{16}\text{O}$ reaction. The γ rays detected as having weak intensities in the spectra gated by the recoiling ions were confirmed to form the low-energy level scheme reported in Ref. [6] up to the $E_x = 1195.4$ keV level.

The strong 809.0, 836.0, and 1192.3 keV γ -rays were found to form a cascade that feeds the 1195.4 keV level. The fact that the transitions below this level (198, 221, 412 keV) are seen with weaker intensities in coincidence with the recoils suggests that the lifetime of the 1195.4 keV level is of the order of a few nanoseconds, comparable to the time intervals needed by the recoils to fly out of the central spatial region, viewed by the CLARA array (note that the 974 keV transition from this level is not visible in these spectra due to its lower detection efficiency—a factor of about 3 lower than that of the 221 keV transition). The lowest panel shown in Fig. 2 is a triple γ -coincidence spectrum obtained by setting double gates on the 197.9 keV γ ray and any of the 809.0 or 836.0 keV γ rays. The level scheme established for ^{89}Rb is shown in Fig. 3 and information concerning the observed γ -ray transitions are given in Table I.

Of particular interest is the spin-parity of the $E_x = 1195.4$ keV level. In the ENSDF database, it was reported as having a spin ($\leq 7/2$) [6]. However, by corroborating the present data with older information, we have arguments that this state has $J^\pi = 9/2^+$. First, one can observe that by using the multiplicities deduced from ADO ratios and presented in Table I, one may assign spins of (7/2), (7/2), and (9/2) to the states at 586.0, 997.5, and 1195.4 keV, respectively. The previous assignment $J \leq 7/2$ in Ref. [6] seems to be mainly based on the fact that a weak branch of its decay to the 3/2⁻ (g.s.) was reported. Nevertheless, it was pointed out that the large $\log ft$ value of 7.78(15) of its β decay feeding from the 3/2⁽⁺⁾ ground state of ^{89}Kr [4,6] disfavors

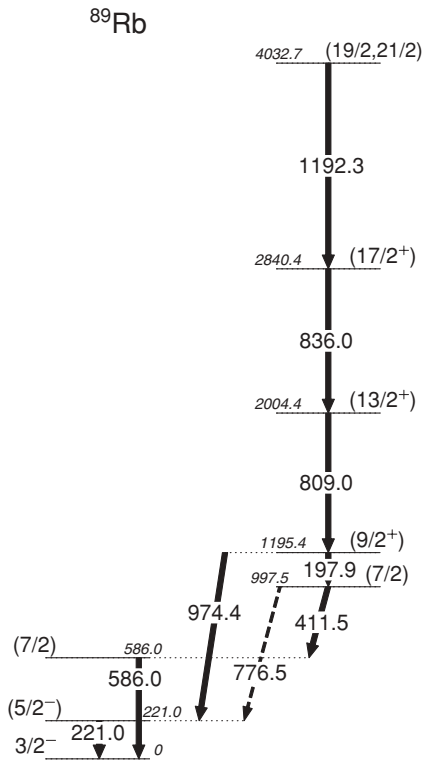


FIG. 3. Level scheme of ^{89}Rb as obtained from the current work. Up to the 1195.4 keV state, the level scheme coincides with that determined in previous studies [6]. Note the $(9/2^+)$ assignment for the 1195.4 keV state, which is a short-lived isomer (lifetime of a few ns, see text). For information on the γ -ray transitions, see Table I.

the $7/2^+$ assignment. However, this state was populated by an $\ell = (3, 4)$ transferred angular momentum in the (α, p) reaction [5], therefore it may be a $9/2^+$ level. Note also that the estimation given above for the lifetime of the 1195-keV level (several nanoseconds) is in agreement with an $M2$ type for the 974 keV transition. The strong population of this state

through the 809–836–1192 keV cascade is another argument in favor of the assignment of this cascade to the positive parity yrast cascade built on the expected $9/2^+$ state in this nucleus when the unpaired proton is excited in the $g_{9/2}$ orbital. Figure 4 shows the evolution of both the excitation energy of the $9/2^+$ state (taken with respect to the lowest $3/2^-$ state in all nuclei), and of the $13/2^+ \rightarrow 9/2^+$ transition energy with the number of neutrons in the Rb isotopes. The latter varies, as expected, like the $2^+ \rightarrow 0^+$ transition energy in the neighboring even-even Sr isotopes. These evolutions are very similar with those found in the Y isotopes (see Fig. 9) and therefore, they additionally support the assignment of $9/2^+$ to the 1195.4 keV state. This assignment is discussed further in the section presenting the main results of the shell-model calculations.

B. The ^{92}Y nucleus

The γ rays assigned as transitions in ^{92}Y can be seen in the two upper spectra presented in Fig. 5. These γ -ray spectra were gated on the ^{92}Y mass peaks from Fig. 1. Double gates on the $\gamma\gamma\gamma$ coincidence cube showed that the 185.0, 717.1, 1022.8, 1026.5, and 1096.5 keV γ rays form a cascade because they were found in mutual coincidence relationship in all combinations of double gates. An example of summed double-gated spectrum is shown in the bottom panel of Fig. 5. The resulting level scheme deduced from these coincidence relationships and the transition intensities is shown in Fig. 6. None of these γ transitions in ^{92}Y were previously known. The multiplicities of the transitions presented also in Table I are indicated in the figure suggesting a spin sequence like $J, J + 1, J + 3, J + 4, J + 6, \dots$, where J is the spin of the lowest level of an unknown excitation energy marked as “x.” In the shell-model section, the comparison among the ^{92}Y nucleus, its ^{94}Nb isotone, and the shell-model predictions is presented in detail and it suggests that the lowest state is a (6^+) state, and therefore we may have observed the sequence of levels $(6^+), (7^+), (9^+), (10^+)$, etc.

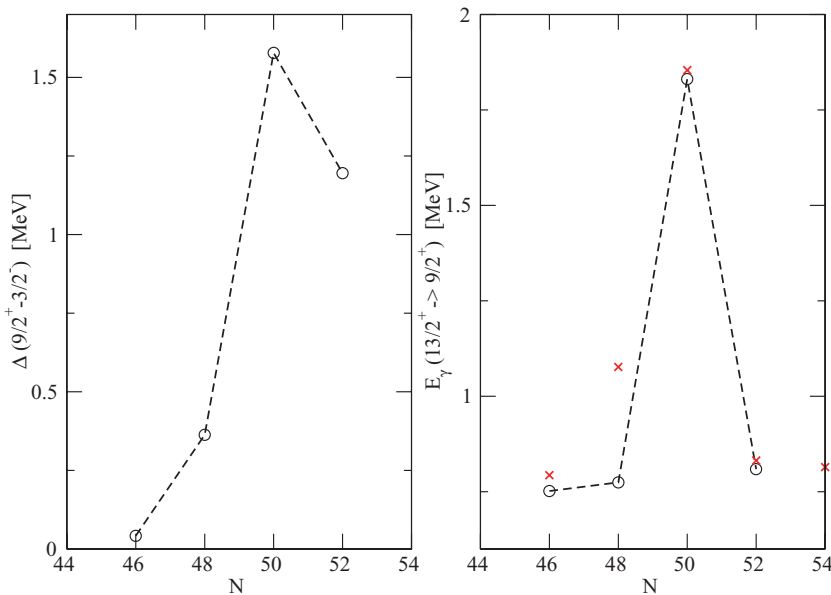


FIG. 4. (Color online) (Left) Energy of the lowest $9/2^+$ state in Rb isotopes, relative to the lowest $3/2^-$ state (which is ground state in all isotopes except ^{85}Rb , where it has 151.2 keV excitation). (Right) The $13/2^+ \rightarrow 9/2^+$ transition energy in the Rb isotopes around $N = 50$, compared with the $2_1^+ \rightarrow 0_1^+$ transition energy in the neighboring Sr cores, represented by “x.”

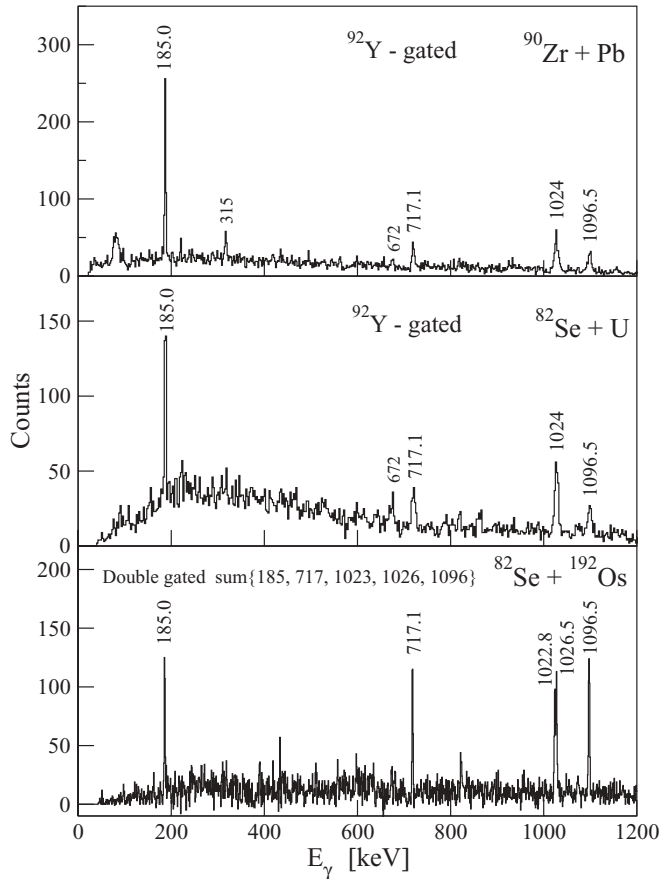


FIG. 5. Same as Fig. 2, but for the ^{92}Y nucleus. The level scheme built from these data is shown in Fig. 6.

C. The ^{93}Y nucleus

The γ rays identified as transitions in ^{93}Y can be observed in the two upper spectra displayed in Fig. 7. These γ -ray spectra were obtained by gating on the ^{93}Y mass peaks shown in Fig. 1. The transitions at energies of 291.4, 677.2, 722.6, 791.7, and 1072.4 keV were placed in the level scheme as shown in Fig. 8. Because it is a rather strongly populated cascade, it was assigned to the positive-parity sequence starting from the $E_x = 758.7$ keV isomeric level, with $J^\pi = 9/2^+$ (the spin assignment of this level in Ref. [14] is erroneous, as correctly pointed out also in Ref. [22]). The tentative J^π assignments in Fig. 8 are based on the multiplicities given in Table I. Figure 9 shows the evolutions of the excitation energy of the $9/2^+$ state (in all these isotopes the ground state is $1/2^-$ therefore it has the same configuration) and of the energy of the first quadrupole transition in the positive-parity yrast sequence versus the number of neutrons. As remarked earlier, there is a similarity to the situation observed in the Rb isotopes (see Fig. 4).

IV. COMPARISON WITH SHELL MODEL CALCULATIONS

To explain the observed structures, spherical shell-model calculations have been performed with the code OXBASH

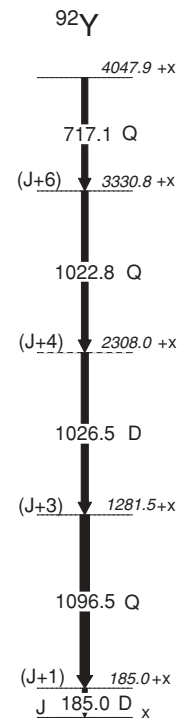


FIG. 6. Level scheme of ^{92}Y as determined in the present work. Multiplicities of transitions are indicated: D, dipole; Q, quadrupole (see Table I). The excitation energy “ x ” of the lowest level is not known. A possible spin-parity assignment for the lowest level is $J^\pi = 6^+$ and the observed cascade may continue with some positive-parity states (see text).

[23]. The residual interaction named “gwbxg” in the code and the corresponding “gwb” model space were used to calculate the excitation energies of the states of interest and the electromagnetic transition probabilities between them. The “gwb” model space includes four valence proton orbitals ($1f_{5/2}$, $2p_{3/2}$, $2p_{1/2}$, and $1g_{9/2}$) and six valence neutron orbitals ($1g_{9/2}$, $2p_{1/2}$, $2d_{5/2}$, $1g_{7/2}$, $3s_{1/2}$, and $2d_{3/2}$). The residual interaction set contains a combination of calculated and empirical two-body matrix elements described in the code (details concerning this interaction are given in Ref. [20]). The electromagnetic decay transition probabilities were calculated using as the effective gyromagnetic factors the classical values of free nucleons and as the effective charges the values of 1.5 and 0.5 for the proton and neutron, respectively.

Due to the large dimensions of the valence space, in the calculations for all three nuclei only up to three particles (protons and/or neutrons) were allowed to be excited from the low-energy orbitals, $f_{5/2}$, $p_{3/2}$, $d_{5/2}$, into the higher-energy ones, $g_{9/2}$, $p_{1/2}$, $g_{7/2}$, $d_{3/2}$, $s_{1/2}$. Also, the $1g_{9/2}$ and $2p_{1/2}$ neutron orbitals were constrained to be fully occupied. The $s_{1/2}$ and $d_{3/2}$ single-particle energies for the neutrons were slightly modified, as described in detail in Ref. [20].

We discuss first the two odd-mass nuclei, ^{89}Rb and ^{93}Y , and then the odd-odd nucleus ^{92}Y . Additional calculations were carried out for the ^{94}Nb nucleus [24] with the goal of extracting some useful information from the comparison of

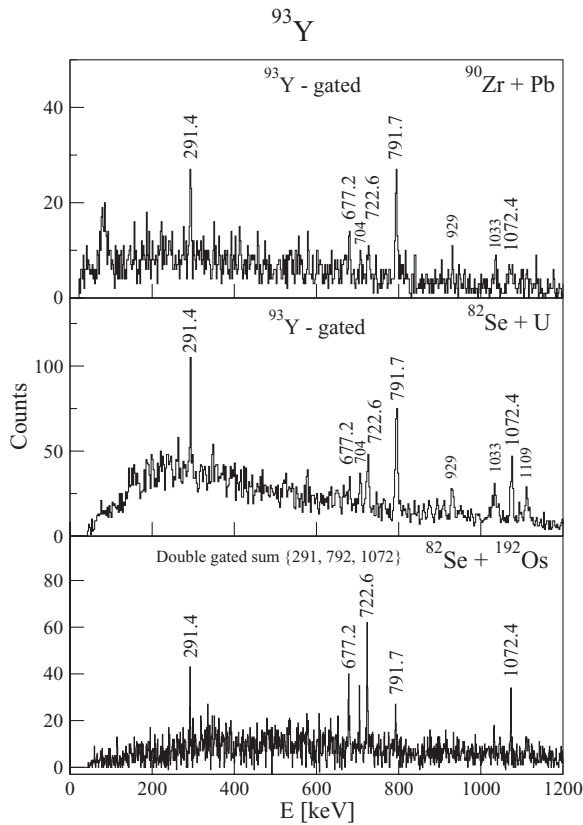


FIG. 7. Same as Fig. 2 but for ^{93}Y . The level scheme built from these data is shown in Fig. 8.

the experimental data and the shell-model predictions of both $N = 53$ isotones ^{92}Y and ^{94}Nb .

A. ^{89}Rb

Figure 10 shows the comparison between the observed level scheme and the shell-model predictions for ^{89}Rb . In the calculated level scheme, the γ -ray transitions are labeled by their relative calculated branching ratios. The orbital occupancies provided by the shell-model calculations are given in Table II. The low-lying negative parity states are well reproduced. The comparison with the calculation suggests that the two $(7/2)$ states at 586 and 998 keV may have negative parity. The lowest negative-parity states, $5/2^-$, $9/2^-$, $13/2^-$, have a dominant simple structure resulting from the coupling of a $f_{5/2}$ proton to a pair of $d_{5/2}$ neutrons coupled to spins 0, 2, and 4. The calculations predict that up to the spin $13/2$ the yrast states are of negative parity, whereas above this value the positive-parity states become yrast. As discussed in the previous section, there are arguments in favor of the positive-parity assignment for the observed states above 1 MeV. Both the energy of the positive-parity states relative to the negative-parity ones and the positive-parity yrast states above the $9/2^+$ isomer are reasonably well predicted by the calculations. Because the $19/2^+$ and $21/2^+$ states lie close to each other and the $19/2^+$ state decays predominantly to the $17/2^+$ state, one cannot unambiguously assign the spin of the highest state observed at 4033 keV.

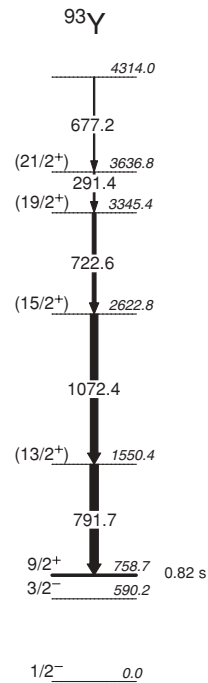


FIG. 8. Level scheme of ^{93}Y as determined from the present work.

B. ^{93}Y

The comparison of the experimental level scheme and the shell model predictions for ^{93}Y is shown in Fig. 11. Unlike the case of ^{89}Rb , the observed sequence is not a stretched $E2$ cascade. The calculations show indeed that the yrast line follows the sequence $9/2^+$, $13/2^+$, $15/2^+$, then possibly $19/2^+$, which decays predominantly toward the $15/2^+$ state. The calculated dipole transition from $19/2^+$ to $17/2^+$ is very much retarded mainly because the $17/2^+$ and $19/2^+$ lie very close in energy. According to the multiplicities in Table I, the experimental sequence may continue with the $21/2^+$ and $25/2^+$ states, like the theoretical one. At higher spins the agreement deteriorates probably due to the severity of the valence space truncation used in our calculations.

C. ^{92}Y

Figure 12 presents the comparison of the calculations with the level scheme observed for ^{92}Y . In the same figure, one can see a similar comparison for its isotone ^{94}Nb [24], for which shell-model calculations were performed using the same truncation conditions, the same valence space, and the same residual interaction set.

In ^{94}Nb , the experimental yrast sequence was observed as an irregular cascade on top of a low-energy transition of 79 keV, $(7^+) \rightarrow 6^+$, and some other yrare transitions feeding the same state [24]. We note here that we made a new study of ^{94}Nb based on the triple coincidence data obtained in the $^{82}\text{Se} + ^{192}\text{Os}$ experiment and, while largely confirming the level scheme assigned in Ref. [24], this new study showed that some changes are necessary. In the low-energy part of interest here, the order of the 869 to 983 keV cascade de-exciting a level at 1931 keV [24] to the 79 keV 7^+ state was reverted and

TABLE II. Occupation numbers of the spherical orbitals from the shell-model calculations. Note that the $N = 50$ core was not broken in these calculations (the neutron $1g_{9/2}$ and $2p_{3/2}$ orbitals are fully occupied).

State		Protons					Neutrons				
E_x (keV)	J^π	$1f_{5/2}$	$2p_{3/2}$	$2p_{1/2}$	$1g_{9/2}$	$2p_{1/2}$	$1g_{9/2}$	$1g_{7/2}$	$2d_{5/2}$	$2d_{3/2}$	$3s_{1/2}$
⁸⁹ Rb											
0	3/2 ⁻	5.745	2.732	0.446	0.077	2.000	10.000	0.009	1.757	0.053	0.181
549	1/2 ⁻	5.666	2.346	0.909	0.079	2.000	10.000	0.011	1.801	0.062	0.126
173	5/2 ⁻	5.053	3.303	0.517	0.126	2.000	10.000	0.008	1.785	0.046	0.160
935	7/2 ⁻	5.685	2.724	0.502	0.089	2.000	10.000	0.004	1.884	0.046	0.065
1153	7/2 ⁻	4.935	3.404	0.505	0.157	2.000	10.000	0.006	1.721	0.040	0.233
1336	9/2 ⁺	4.622	2.866	0.471	1.041	2.000	10.000	0.010	1.790	0.039	0.160
2234	11/2 ⁺	4.674	2.777	0.510	1.039	2.000	10.000	0.007	1.866	0.025	0.103
2490	13/2 ⁺	4.525	3.063	0.371	1.040	2.000	10.000	0.010	1.742	0.049	0.200
3214	15/2 ⁺	4.753	2.783	0.425	1.039	2.000	10.000	0.007	1.826	0.032	0.135
3070	17/2 ⁺	4.668	2.810	0.476	1.046	2.000	10.000	0.008	1.877	0.069	0.046
4387	19/2 ⁺	4.798	2.756	0.415	1.031	2.000	10.000	0.014	1.820	0.091	0.074
4344	21/2 ⁺	4.655	2.932	0.381	1.033	2.000	10.000	0.024	1.765	0.192	0.019
5205	23/2 ⁺	4.737	2.856	0.375	1.033	2.000	10.000	0.026	1.805	0.138	0.031
5694	25/2 ⁺	5.095	2.515	0.389	1.000	2.000	10.000	0.996	1.000	0.003	0.000
⁹² Y											
0	2 ⁻	5.970	3.776	1.090	0.165	2.000	10.000	0.007	2.839	0.067	0.086
407	3 ⁻	5.967	3.804	1.048	0.181	2.000	10.000	0.009	2.828	0.073	0.091
950	4 ⁻	5.968	3.704	1.153	0.174	2.000	10.000	0.004	2.914	0.068	0.014
824	3 ⁺	5.731	3.481	0.724	1.064	2.000	10.000	0.011	2.657	0.252	0.080
1061	4 ⁺	5.736	3.501	0.697	1.066	2.000	10.000	0.014	2.700	0.139	0.147
1011	5 ⁺	5.735	3.577	0.614	1.074	2.000	10.000	0.009	2.501	0.057	0.433
1047	6 ⁺	5.711	3.521	0.700	1.067	2.000	10.000	0.013	2.774	0.125	0.088
1522	7 ⁺	5.742	3.517	0.677	1.064	2.000	10.000	0.011	2.769	0.122	0.098
2307	8 ⁺	5.752	3.453	0.721	1.075	2.000	10.000	0.949	2.005	0.025	0.021
2460	9 ⁺	5.692	3.588	0.642	1.079	2.000	10.000	0.017	2.623	0.134	0.225
3395	10 ⁺	5.715	3.552	0.654	1.079	2.000	10.000	0.426	2.005	0.551	0.018
4090	11 ⁺	5.724	3.588	0.598	1.090	2.000	10.000	0.989	1.961	0.009	0.040
3779	12 ⁺	5.702	3.569	0.636	1.093	2.000	10.000	0.995	1.988	0.018	0.000
5730	13 ⁺	5.841	2.967	1.180	1.012	2.000	10.000	1.000	2.000	0.000	0.000
6522	14 ⁺	5.633	3.098	1.254	1.015	2.000	10.000	0.999	2.000	0.001	0.000
⁹³ Y											
0	1/2 ⁻	5.973	3.847	1.048	0.132	2.000	10.000	0.014	3.700	0.122	0.164
642	3/2 ⁻	5.967	3.794	1.086	0.153	2.000	10.000	0.007	3.777	0.084	0.131
943	5/2 ⁻	5.967	3.811	1.060	0.162	2.000	10.000	0.008	3.756	0.096	0.140
1163	7/2 ⁻	5.970	3.761	1.125	0.144	2.000	10.000	0.008	3.849	0.082	0.061
1342	9/2 ⁺	5.725	3.587	0.634	1.054	2.000	10.000	0.016	3.649	0.194	0.141
2234	11/2 ⁺	5.727	3.559	0.655	1.059	2.000	10.000	0.012	3.405	0.230	0.353
1777	13/2 ⁺	5.681	3.591	0.666	1.063	2.000	10.000	0.013	3.565	0.107	0.315
2769	15/2 ⁺	5.707	3.519	0.719	1.055	2.000	10.000	0.040	3.295	0.420	0.245
3164	17/2 ⁺	5.692	3.509	0.742	1.058	2.000	10.000	0.016	3.681	0.155	0.148
3240	19/2 ⁺	5.704	3.499	0.730	1.067	2.000	10.000	0.993	2.985	0.015	0.008
3883	21/2 ⁺	5.703	3.504	0.724	1.069	2.000	10.000	0.912	2.986	0.093	0.008
4960	23/2 ⁺	5.707	3.457	0.772	1.063	2.000	10.000	0.992	2.983	0.018	0.007
4818	25/2 ⁺	5.681	3.606	0.635	1.078	2.000	10.000	0.990	2.958	0.021	0.031

the 983 keV transition is now placed below the 869 keV one. This change is also confirmed by a newly observed crossover transition of 1061 keV decaying the intermediate level directly to the 6⁺ ground state. Consequently, the (8⁺) state is now placed at a higher energy of 1061 keV, above the (9⁺) state at 991 keV. The shell-model calculations for

⁹⁴Nb describe reasonably well the known experimental levels of both parities.

A low-energy transition of 185 keV is placed at the base of the observed cascade in ⁹²Y. This situation is rather similar with that found in ⁹⁴Nb where the low-energy transition of 79 keV ends the decaying yrast sequence. The shell-model

^{93}Y

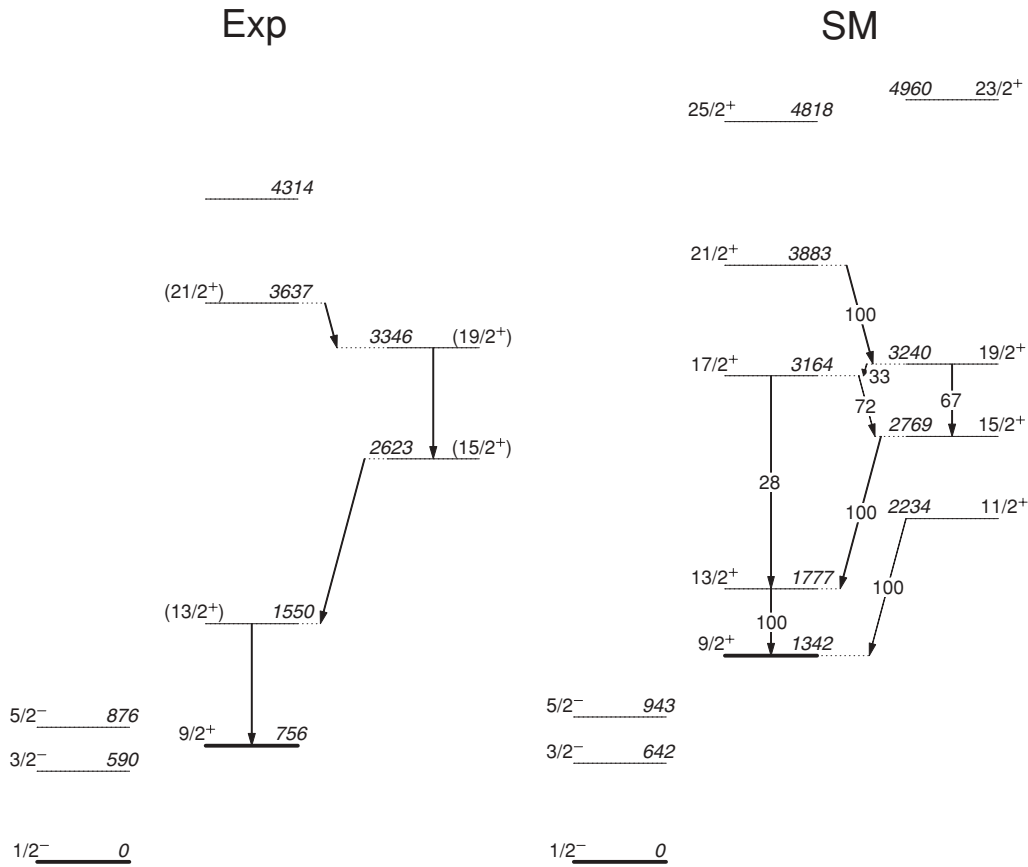


FIG. 11. Comparison between the experimental level scheme of the ^{93}Y nucleus and the shell-model calculations. The calculated electromagnetic transitions are labeled with their relative branching ratios.

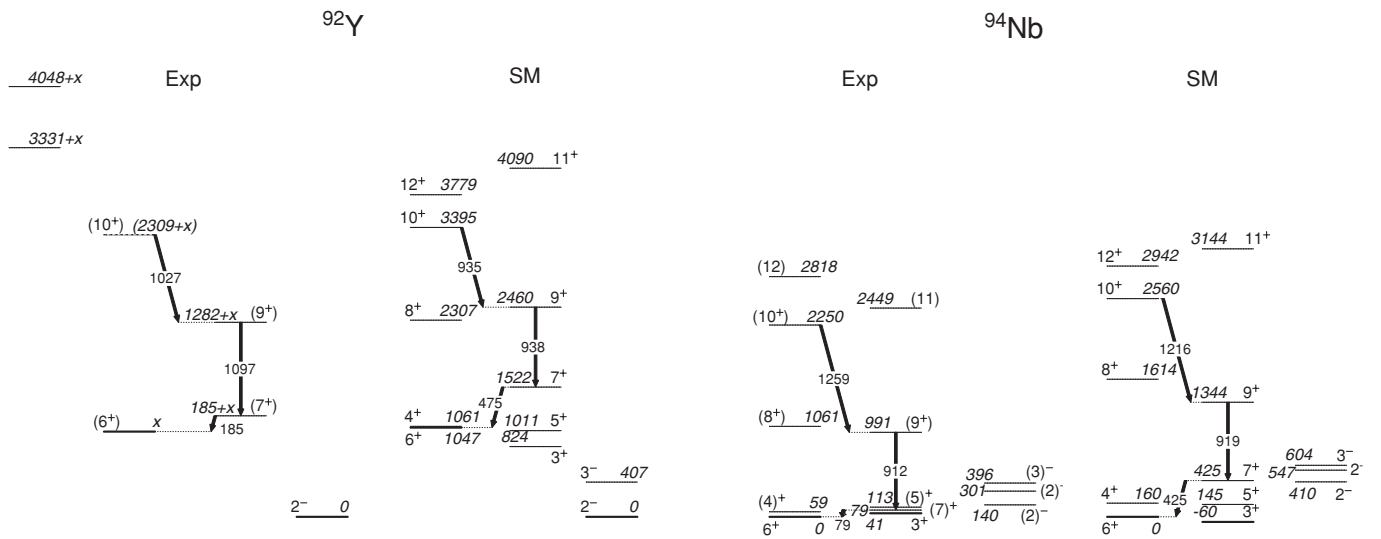


FIG. 12. Comparison between the experimental level schemes of ^{92}Y and ^{94}Nb and the shell-model calculations performed in this work. The indicated spin-parity assignments for the experimental levels of ^{92}Y are tentative, as suggested by these comparisons (see text for details).

in the cascade, as determined by the multipolarities given in Table II, show clear similarities to the ^{94}Nb case where the 10^+ state decays to the 9^+ state and then to the 7^+ one with connecting transitions of about 1000–1200 keV. In good accordance with the experimental data, the shell-model calculations predict similar decay patterns for these states in both nuclei. Higher up, it is difficult to extend both the similarity with ^{94}Nb and the comparison with the calculated spectrum. Both the truncation used and the lack of the high- j orbital ($1h_{11/2}$) make the calculations in the *gwb* space less realistic at relatively large excitation energies. For example, because $h_{11/2}$ has a high spin value, by coupling an unpaired $h_{11/2}$ neutron with an unpaired $g_{9/2}$ proton and eventually with the spin of one pair of neutrons in $d_{5/2}$ with spins 0, 2, or $4\hbar$, negative-parity states with total spins in the range of 10– $14\hbar$ may be generated rather close to, or even along the yrast line.

V. CONCLUSIONS

Positive-parity yrast decay sequences were identified in ^{89}Rb , ^{92}Y , and ^{93}Y by combining the results of two multinucleon transfer reaction experiments with those obtained from a fusion-evaporation reaction. In the multinucleon transfer reaction experiments, several previously unknown γ -ray transitions were detected in coincidence with the

recoiling nuclei ^{89}Rb , ^{92}Y , and ^{93}Y . Starting from these newly identified transitions, the level schemes of these nuclei were constructed by analyzing the triple γ -ray coincidence data acquired in a thick target experiment. The observed structures contribute to the experimental data systematics of the nuclei with $N = 52, 53$, and 54.

Shell-model calculations were performed for all nuclei with the OXBASH shell-model code using the *gwb* configuration space ($\pi f_{5/2}, \pi p_{3/2}, \pi p_{1/2}, \pi g_{9/2}, \nu p_{1/2}, \nu g_{9/2}, \nu d_{5/2}, \nu g_{7/2}, \nu s_{1/2}$, and $\nu d_{3/2}$) and the *gwbxg* residual interaction. The neutron $2p_{1/2}$ and $1g_{9/2}$ orbitals were kept fully occupied and only up to three nucleons were allowed to be excited from the low-energy orbitals, $f_{5/2}, p_{3/2}$, and $d_{5/2}$, into the higher-energy ones, $g_{9/2}, p_{1/2}, g_{7/2}, d_{3/2}$, and $s_{1/2}$. With these truncations, the calculations describe reasonably well the observed level schemes up to medium-high spin values of 10– $11\hbar$.

ACKNOWLEDGMENTS

We acknowledge support received within the FP6 European Contract EURONS n RII3-CT-2004-506065-V Framework Programme. This work was partially funded by EPSRC(UK) and by the Romanian Ministry for Education and Research under contract no. CEX-05-D11-30.

-
- [1] Y. H. Zhang *et al.*, Phys. Rev. C **70**, 024301 (2004).
 - [2] G. A. Jones *et al.*, Phys. Rev. C (in press).
 - [3] P. H. Regan *et al.*, AIP Conf. Proc. **819**, 464 (2006).
 - [4] E. A. Henry, W. L. Talbert, Jr., and J. R. McConnel, Phys. Rev. C **7**, 222 (1973).
 - [5] G. S. F. Stephans, Diss. Abst. Int. B **43**, 3640 (1983), as quoted in Ref. [6].
 - [6] B. Singh, Nucl. Data Sheets **85**, 1 (1998).
 - [7] A. E. Norris and A. C. Wahl, Phys. Rev. **146**, 926 (1966).
 - [8] K. Suzuki, J. Kawa, and K. Okada, Nucl. Phys. **A228**, 513 (1974).
 - [9] C. M. Baglin, Nucl. Data Sheets **91**, 423 (2000).
 - [10] C. J. Bischof and W. L. Talbert, Jr., Phys. Rev. C **15**, 1047 (1977); E. Achterberg *et al.*, Phys. Rev. C **10**, 2526 (1974).
 - [11] V. R. Casella, J. D. Knight, and R. A. Naumann, Nucl. Phys. **A239**, 83 (1975).
 - [12] B. M. Preedom, E. Newman, and J. C. Hiebert, Phys. Rev. **166**, 1156 (1968).
 - [13] R. J. Peterson and H. Rudolph, Nucl. Phys. **A241**, 253 (1975).
 - [14] C. M. Baglin, Nucl. Data Sheets **80**, 1 (1997).
 - [15] A. M. Stefanini *et al.*, Nucl. Phys. **A701**, 217c (2002).
 - [16] A. Gadea *et al.*, Eur. Phys. J. A **20**, 193 (2004).
 - [17] S. Szilner *et al.*, Phys. Rev. C **76**, 024604 (2007).
 - [18] L. Corradi *et al.*, Nucl. Phys. **A787**, 160c (2007).
 - [19] Zs. Podolyák *et al.*, Int. J. Mod. Phys. E **13**, 123 (2004).
 - [20] D. Bucurescu *et al.*, Phys. Rev. C **71**, 034315 (2005).
 - [21] D. Bazzacco, Proceedings of the International Conference of Nuclear Structure at High Angular Momentum, Ottawa, 1992 [Report No. AECL 10613], Vol. II, 376.
 - [22] B. Cheal *et al.*, Phys. Lett. **B645**, 133 (2007).
 - [23] B. A. Brown, A. Etchegoyen, W. D. M. Rae, and N. S. Godwin, Computer Code OXBASH, MSU NSCL Report No. 524, 1984 (unpublished).
 - [24] N. Mărginean, D. Bucurescu, G. Cata-Danil, I. Cata-Danil, M. Ivascu, and C. A. Ur, Phys. Rev. C **62**, 034309 (2000).